Table I. Axial (R_{ax}) and Equatorial (R_{eq}) Optimized Bond Lengths (Å) of the Radicals and Anions of Planar XH_3 and Hypercoordinated XH_5 Species (X = C, Si)[a]

	SiH_5^-	$SiH_5^\bullet$	$SiH_3^\bullet$	SiH_3^-	CH_5^-	$CH_5^\bullet$	$CH_3^\bullet$	CH_3^-
R_{ax}	1.625	1.589			1.692	1.337		
R_{eq}	1.521	1.488	1.460	1.471	1.062	1.079	1.072	1.076

[a] The radicals have been calculated with the RHF open-shell Davidson Hamiltonian.[7]

structures only,[2a] as shown in Figure 2. The major consequential change arises in the energy of the species, which, as schematized in **2**, is converted to a high-energy transition state relative to its normal coordinated species.

Let us turn to discuss the carbon analogues. As shown previously,[1h] the hypercoordinated structure Ψ_{HC} is so stable owing to (a) the good overlap capability of the a_s' σ^* orbital of the SiH_3 fragment with an axial hydrogen, and to (b) the low promotion energy required to populate the $\sigma^*(SiH_3)$ orbital and prepare it thereby for bonding. In CH_5^-, on the other hand, the a_s' $\sigma^*(CH_3)$ orbital is too high in energy and overlaps too weakly with an axial ligand to be able to stabilize efficiently a structure like Ψ_{HC}. Consequently, CH_5^- remains a transition state just like $CH_5^\bullet$. In conclusion, $SiH_5^\bullet$, CH_5^-, and $CH_5^\bullet$ are described by the same bonding mechanism, the resonance hybrid of the Lewis structures, as in **2**, which differs from the hypercoordinated bonding mechanism of SiH_5^- in Figure 1B and in **1**.

It is interesting to examine the coherence of the above-described bonding mechanisms in the geometric features of the radicals and anions of CH_5 and SiH_5. First, the axial bond lengths of CH_5^- are expected to be longer than those of $CH_5^\bullet$, since four electrons undergo more exchange repulsion than three in the axial three-orbital system, much like H_3^- having longer H-H bond lengths[5] than $H_3^\bullet$. Second, the equatorial C-H bond lengths for CH_5^- and $CH_5^\bullet$ should be almost identical, and roughly equal to the C-H bond lengths of planar CH_3^- or $CH_3^\bullet$.

On the other hand, the dominance of Ψ_{HC} in the wave function of SiH_5^- leaves only three electrons in the axial three-orbital system, just as in the $SiH_5^\bullet$ radical, so that no significant lengthening of the axial bonds is expected as an electron is added to $SiH_5^\bullet$. Moreover, while the equatorial bonds of $SiH_5^\bullet$ are expected to be close to those of the planar SiH_3^- or $SiH_3^\bullet$ species, the equatorial bonds of SiH_5^- are expected to be significantly longer since their antibonding σ^* orbital is populated in the Ψ_{HC} structure.

To verify these qualitative arguments, we have optimized the geometries of $SiH_5^\bullet$, SiH_5^-, $CH_5^\bullet$, CH_5^-, $SiH_3^\bullet$, SiH_3^-, $CH_3^\bullet$, and CH_3^- at a consistent level of theory, ab initio Hartree-Fock with the 6-31++G** basis set,[6] including polarization functions and diffuse orbitals on all atoms. The results, displayed in Table I, nicely confirm all of the above expected tendencies and are as follows: (i) The equatorial bond lengths exhibit no significant differences in the bonding types of $SiH_5^\bullet$ and $CH_5^\bullet$, being close to the bond lengths of the planar XH_3 species. On the other hand, while the equatorial bond lengths are slightly *shorter* in CH_5^- relative to CH_3, the same bonds are *longer* in SiH_5^- relative to SiH_3. While the lengthening (0.050-0.061 Å) may seem to be modest, it should be remembered that, in the hypercoordinated structure Ψ_{HC}, only one equatorial σ^* orbital (the a_s' combination) out of the available three is populated. (ii) While the C-H axial bond lengths increase by 0.355 Å from $CH_5^\bullet$ to CH_5^-, the corresponding increase in the Si-H bond lengths is an order of magnitude less, only 0.036 Å, from $SiH_5^\bullet$ to SiH_5^-. The effect of Ψ_{HC} on SiH_5^- is so profound that the axial Si-H distance ends up being *shorter* than the corresponding C-H distance.

In summary, hypercoordination in SiH_5^- is an efficient delocalization mechanism of the 10-electron/6-center type. This efficient mechanism is made possible by a hypercoordinated resonance structure, Ψ_{HC}, whose involvement allows delocalization of the fifth electron pair into both axial and equatorial Si-H bonds in SiH_5^-. Removal of one electron results also in the disappearance of this hypercoordinated configuration and generates an unstable $SiH_5^\bullet$ species in which electron delocalization is restricted to the axial H···Si···H linkage which is the conventional three-electron/three-center delocalized system. While the analogy between $SiH_5^\bullet$ and $CH_5^\bullet$ holds, SiH_5^- with its Ψ_{HC} structure displays very different bonding features from CH_5^- and this is reflected in both energetic and geometric features of these species. It should be noted that other arguments have been put forward by Gronert, Glaser, and Streitwieser,[8] who explained the stability of SiH_4F^- by the importance of ionic contributions to bonding. We do not believe, however, that the ionic model can be extended to the SiH_5^- case. Indeed, all the ionic contributions are included, with their optimized coefficients, in our calculations of Lewis structures, and despite this, SiH_5^- is not found to be stable in the absence of the hypercoordinated Ψ_{HC} structure.[1h,i]

Acknowledgment. This research was supported by the Basic Research Foundation, administrated by the Israel Academy of Sciences and Humanities.

(5) For H_3^-, see: (a) Hirao, K.; Yamabe, S. *Chem. Phys.* **1983**, *80*, 237. (b) Rayez, J. C.; Rayez-Meaume, M. T.; Massa, L. *J. Chem. Phys.* **1981**, *75*, 5393. (c) Michels, H. M.; Montgomery, J. A. *Chem. Phys. Lett.* **1987**, *139*, 535. (d) For $H_3^\bullet$, see: Liu, B. *J. Chem. Phys.* **1973**, *58*, 1925.

(6) For first-row elements: Hehre, W. J.; Ditchfield, R.; Pople, J. A. *J. Chem. Phys.* **1972**, *56*, 2257. Hariharan, P. C.; Pople, J. A. *Theor. Chim. Acta* **1973**, *28*, 213. For second-row elements: Francl, M. M.; Pietro, W.; Hehre, W. J.; Binkley, J. S.; Gordon, M. S.; DeFrees, D. J.; Pople, J. A.; *J. Chem. Phys.* **1982**, *77*, 3654. Gordon, M. S.; Binkley, J. S.; Pople, J. A.; Pietro, W. J. *J. Am. Chem. Soc.* **1982**, *104*, 2797.

(7) Davidson, E. R. *Chem. Phys. Lett.* **1973**, *21*, 565.

(8) Gronert, S.; Glaser, R.; Streitwieser, A. *J. Am. Chem. Soc.* **1989**, *111*, 3111.

Contribution from the Laboratoire de Chimie Inorganique, URA No. 420, Université de Paris-Sud, 91405 Orsay, France

Single-Crystal EPR Study of Copper(II) Trinuclear Compounds: Exchange-Averaging Effects

Yves Journaux,* Francisco Lloret,[1] and Olivier Kahn*

Received August 2, 1989

Three years ago, we described two copper(II) trinuclear compounds with dithiooxamide derivative ligands.[2] Their formula is $\{Cu_3[C_2S_2(NCH_2CH_2CH_2SCH_2CH_2OH)_2]_2\}X_2$ with X = ClO_4 (**1**) and NO_3 (**2**). The crystal structure of **1** has been solved and is recalled in Figure 1. It consists of trinuclear cations and noncoordinated perchlorate anions. The central copper atom is in a square-planar CuS_4 chromophore, and the terminal copper atoms are in $CuS_2N_2O_2$ chromophores with a 4 + 2 coordination. The crystal structure of **2** has not been properly refined because of a disorder of the lateral chains of the dithiooxamide derivatives. The available crystal data, however, indicate that the molecular structure of the trinuclear cation is very similar to that found in **1**. The central copper atom in **2**, however, is located on an inversion center. As far as the packings are concerned, both compounds have S···S intermolecular contacts of the order of 3.5 Å.

The magnetic properties for **1** and **2**, measured in the 50-300 K temperature range, have revealed a strong intramolecular antiferromagnetic interaction between nearest-neighbor copper(II) ions.[2] The doublet ground state is stabilized by ca. 480 and 720 cm^{-1} with regard to the doublet and quartet excited states, re-

(1) Permanent address: Department of Inorganic Chemistry, University of Valencia, Spain.

(2) Veit, R.; Girerd, J. J.; Kahn, O.; Robert, F.; Jeannin, Y. *Inorg. Chem.* **1986**, *25*, 4175.

0020-1669/90/1329-3048$02.50/0

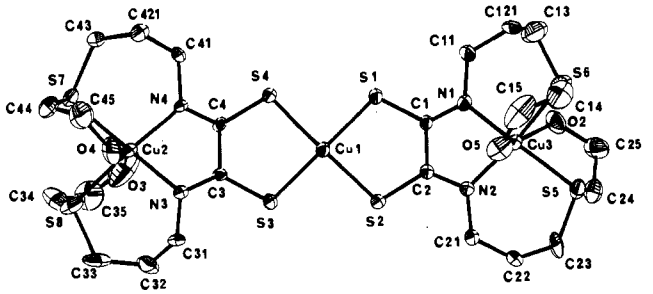

Figure 1. Perspective view of the trinuclear cation $[Cu_3(C_2S_2(NCH_2CH_2CH_2SCH_2CH_2OH)_2)_2]^{2+}$ in **1**.

spectively. Below ca. 200 K, only the ground doublet state is thermally populated and accordingly the magnetic susceptibility χ_M follows a Curie law. The X-band powder EPR spectrum of **2** has also been recorded. From the local symmetry of the interacting metal ions and the molecular symmetry as a whole, the rhombicity of the molecular **g** tensor associated with the doublet ground state is expected to be very weak, with $g_{zz} \gg g_{xx} \simeq g_{yy}$. In fact, below 150 K, the spectrum for **2** exhibits the features characteristic of a strong rhombic distortion. To understand the EPR properties of this species, we decided to carry out a single-crystal investigation. This note is devoted to this study.

Experimental Section

Crystallographic Information. **1** and **2** were synthesized as previously described. Well-shaped single crystals were obtained by slow evaporation from a methanolic solution. The perchlorate compound **1** crystallizes in the orthorhombic system, space group *Pbca*. The lattice parameters are $a = 15.638$ (6) Å, $b = 18.254$ (9) Å, and $c = 29.437$ (7) Å with $Z = 8$. The nitrate compound **2** crystallizes in the monoclinic system, space group $P2_1/c$, with the lattice parameters $a = 14.787$ Å, $b = 14.883$ Å, $c = 9.579$ Å, $\beta = 106.19°$, and $Z = 2$ (trinuclear unit).

EPR Spectra. The EPR study was carried out at X-band frequency by using a Bruker ER 200D spectrometer equipped with a helium continuous-flow cryostat built by Oxford Instruments. The spectra were recorded at 8 K with a crystal fixed on a Perpex rod able to rotate around the vertical axis. The axis of the rod was set perpendicular to the studied plane. The angular dependence of the lines was determined in three different planes for each compound, namely the (100), (010), and (001) planes for **1** and the (001), (1$\bar{1}$0), and (110) planes for **2**. For each plane, the angular variation of g_{eff}^2 was expressed as

$$g_{eff}^2 = g_{ii}^2 \cos^2\theta + 2g_{ij}^2 \sin\theta\cos\theta + g_{jj}^2 \sin^2\theta \qquad (1)$$

where θ is the angle between the magnetic field and a direction taken as the origin. As usual, g_{eff} is deduced from the resonant field. Least-squares fitting of the experimental data led to the g_{ij} elements of the **g** tensor. The reliability factor was defined as

$$R = \sum[(g_{eff}^2)^{obs} - (g_{eff}^2)^{calc}]^2 / [\sum(g_{eff}^2)^{obs}]^2$$

For the nitrate compound **2**, the three studied planes were not orthogonal, and to determine the principal values and directions of **g**, we used a method derived from that proposed by Byrn and Strouse.[3] This method consists of utilizing five different frames, namely the direct and reciprocal lattice frames, the laboratory frame (a, b, c^*), and the direct and reciprocal EPR frames. The direct EPR frame was defined by the (001), (1$\bar{1}$0), and (110) rotation axes, and the reciprocal EPR frame was deduced from the direct EPR frame in the usual way. As the rotation axes were known, it was a straightforward procedure to calculate the transformation matrices connecting all these frames. In principle, the **g** tensor could be determined in the direct EPR frame, but it was then difficult to know the angle between the magnetic field and the coordination axes. On the other hand, in the reciprocal EPR frame, two of the coordinate axes belong to the studied plane, which makes much easier the determination of the angles. The general expression of g_{eff}^2 in the reciprocal EPR frame is

$$g_{eff}^2 = (1/\|h\|^2)[g_{ii}^2u^2 + g_{jj}^2v^2 + g_{kk}^2w^2 + 2g_{ij}^2uv + 2g_{jk}^2vw + 2g_{ki}^2wu] \qquad (2)$$

u, v, and w are the coordinates of the magnetic field direction, and $\|h\|$ is the modulus of the magnetic field direction vector in the reciprocal EPR frame. In practice, the **g** tensor was determined in two steps; first, the diagonal elements were obtained by setting ($u = 1$, $v = 0$, $w = 0$), ($u = 0$, $v = 1$, $w = 0$), and ($u = 0$, $v = 0$, $w = 1$) in eq 2 and by calculating the corresponding g_{eff}^2 values through eq 1. Then, the off-diagonal elements were calculated through the relation

$$g_{ij}^2 = [\|h\|^2 g_{eff}^2 - g_{ii}^2 - g_{jj}^2]/2 \qquad (3)$$

g_{eff}^2, deduced from eq 1, corresponds to the situation where the magnetic field lies along the bisector between the reciprocal coordinate axes. Finally, the **g** tensor is expressed in the laboratory frame, by using the usual transformation matrices.

Magnetic Measurements. These were performed with a Faraday type magnetometer equipped with a helium continuous-flow cryostat in the 50–4.2 K temperature range and a laboratory-made low-field SQUID magnetometer below 7 K.

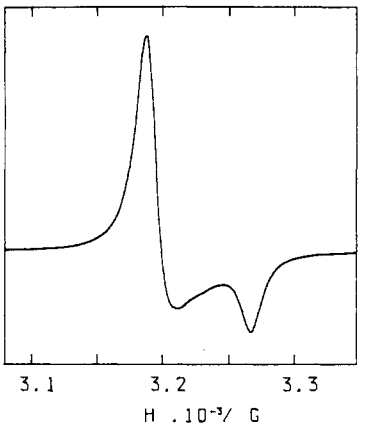

Figure 2. X-Band powder spectrum of **1** at 7.8 K.

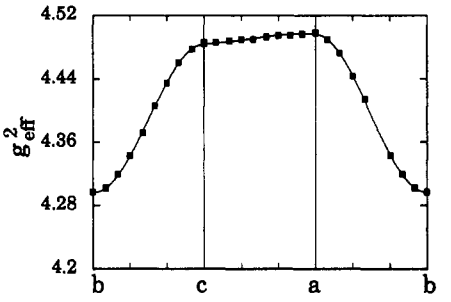

Figure 3. Angular dependence of g_{eff}^2 for **1**: (■) experimental data; (—) calculated variations.

Table I. Principal Values and Directions of the **g** Tensor for **1** with Regard to the $\vec{a}/\|\vec{a}\|$, $\vec{b}/\|\vec{b}\|$, and $\vec{c}/\|\vec{c}\|$ Frame

g	l	m	n
2.121	0.994	-5.1×10^{-3}	−0.100
2.117	0.100	-7.8×10^{-3}	0.994
2.073	5.9×10^{-3}	0.99996	7.2×10^{-3}

Results

Compound 1. The X-band powder spectrum is shown in Figure 2. It presents an axial symmetry with $g_\parallel = 2.072$ and $g_\perp = 2.116$. The angular variations of g_{eff}^2 in the (100), (010), and (001) planes are given in Figure 3. Owing to the orthorhombic symmetry, there are two magnetically nonequivalent magnetic cations in the *ab*, *bc*, and *ac* planes and two lines are expected. In the present case, only one line is observed for any orientation of the crystal. This indicates that the trinuclear species are not perfectly isolated from a magnetic viewpoint. Intermolecular interactions are operative. The experimentally determined principal values and directions of the **g** tensor with regard to the $\vec{a}/\|\vec{a}\|$, $\vec{b}/\|\vec{b}\|$, and $\vec{c}/\|\vec{c}\|$ frame are given in Table I. $\|\vec{a}\|$, $\|\vec{b}\|$, and $\|\vec{c}\|$ are the moduli of the $\vec{a}$, $\vec{b}$, and $\vec{c}$ vectors, respectively. Within the experimental uncertainties (which leads to nonrigorously zero off-diagonal terms), the principal directions of **g** are along the crystal axes as required for exchange-narrowed signals. The largest deviation with respect to this orientation is found in the *ac* plane. This is

(3) Byrn, M. P.; Strouse, C. E. *J. Magn. Reson.* **1983**, *53*, 32.

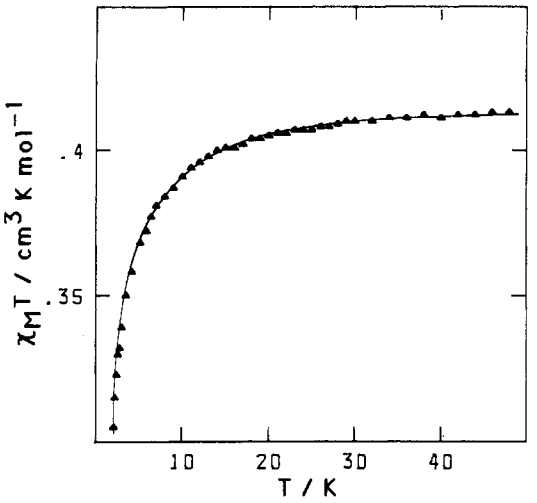

Figure 4. $\chi_M T$ versus T plot for **1** in the 2–50 K temperature range: (▲) experimental points; (—) calculated curve with a Curie–Weiss law.

due to the very small anisotropy of **g** in this plane, which makes difficult the precise determination of the principal directions. The study of the line shapes reveals a Lorentzian behavior, as expected for exchange-narrowing effects. However, since only X-band data are available, the relation between intermolecular interaction parameter J and line width ΔH_{pp} in the high-frequency limit, given by Anderson,[4] is questionable. This relation

$$J \simeq \beta H^2(g_a - g_b)^2/8g_{av}\Delta H_{pp} \qquad (4)$$

in which g_a and g_b are the effective g values in the direction of the applied magnetic field for the nonequivalent magnetic centers and g_{av} is the average value, leads to $J \simeq -0.1$ cm^{-1}.

The temperature dependence of the molar magnetic susceptibility for **1** has been reinvestigated, down to 2 K. As already mentioned, in the 50–200 K temperature range, $\chi_M T$ is constant and equal to what is expected for a magnetically isolated doublet state ($\chi_M T = N\beta^2 g^2/4k$). Below 50 K, $\chi_M T$ decreases more and more rapidly, as shown in Figure 4. Actually, χ_M closely follows a Curie–Weiss law ($\chi_M = C/(T - \Theta)$) with $\Theta = -0.62$ (4) K. This Θ value is obviously related to intermolecular interactions between $S = {}^1/_2$ molecular states. In the mean field approximation, Θ is expressed as[5]

$$\Theta = zJS(S + 1)/3k \qquad (5)$$

where z is the number of nearest neighbors around a given molecule. The interaction Hamiltonian is expressed as $-zJ\langle S_z\rangle S_z$, where $\langle S_z\rangle$ is the mean value of the S_z component of the spin operator. zJ deduced from the Weiss constant is then equal to $-1.7(2)$ cm^{-1}. Each trinuclear species has two rather close neighbors, so that z may be estimated as 2. These two neighbors, however, are not strictly equivalent. Actually, owing to the limitations of the mean field approximation, it is likely preferable to assert that the intermolecular interaction parameter is of the order of the wavenumber, which is about 1 order of magnitude larger than the value estimated from the EPR line width analysis. The value deduced from the magnetic susceptibility data is obviously more reliable. The important point emerging from this magnetic susceptibility study is that, in spite of the separation between the magnetic trinuclear species and the presence of noncoordinated perchlorate anions in the lattice, the intermolecular interactions, although weak, are far from being negligible.

Compound 2. The X-band EPR spectrum of **2** is represented in Figure 5. It presents a rhombic symmetry with $g_1 = 2.062$, $g_2 = 2.102$, and $g_3 = 2.149$. The angular variations of g_{eff}^2 in the (001), (1$\bar{1}$0), and (110) planes are shown in Figure 6. Again, in spite of the presence of two magnetically nonequivalent magnetic sites, a single signal is observed whatever the orientation of the crystal with respect to the magnetic field may be. As for compound **1**, intermolecular interactions are operative. The principal values and directions of **g** with regard to the $\vec{a}/\|\vec{a}\|$, $\vec{b}/\|\vec{b}\|$, and $\vec{c}^*/\|\vec{c}^*\|$ frame are given in Table II. As required for an ex-

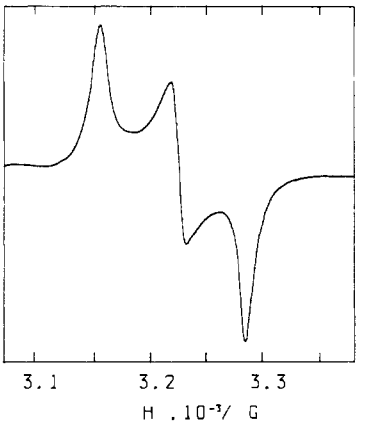

Figure 5. X-Band powder spectrum of **2** at 8.5 K.

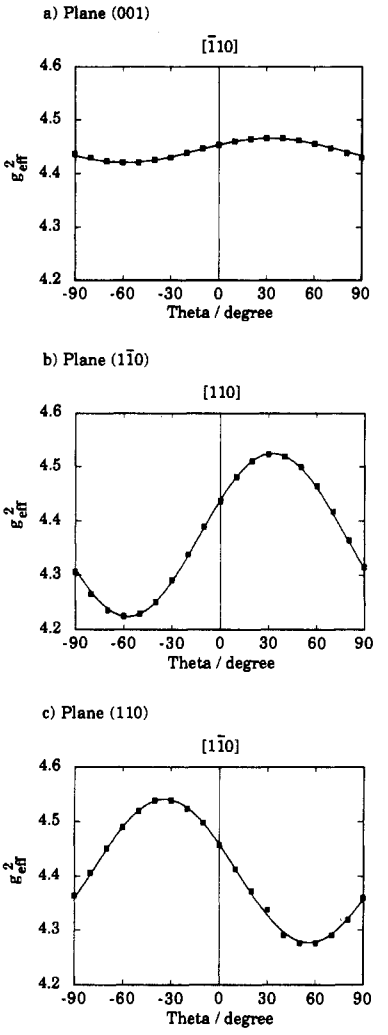

Figure 6. Angular dependence of g_{eff}^2 for **2**: (a) (001) plane; (b) (1$\bar{1}$0) plane; (c) (110) plane; (■) experimental data; (—) calculated variations.

Table II. Principal Values and Directions of the **g** Tensor for **2** with Regard to the $\vec{a}/\|\vec{a}\|$, $\vec{b}/\|\vec{b}\|$, and $\vec{c}^*/\|\vec{c}^*\|$ Frame

g	l	m	n
2.150	0.775	-7.59×10^{-3}	0.632
2.104	−0.039	0.997	0.061
2.056	−0.631	−0.072	0.773

(4) Anderson, P. W. *J. Phys. Soc. Jpn.* **1954**, *9*, 316.
(5) O'Connor, C. J. *Prog. Inorg. Chem.* **1982**, *29*, 203.

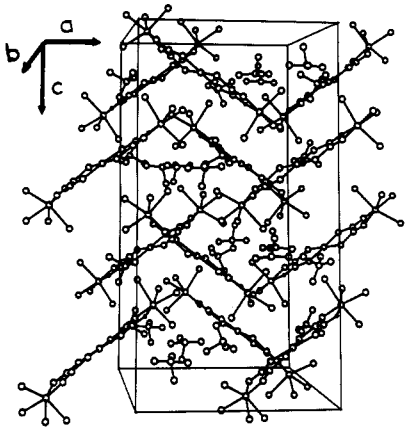

Figure 7. Crystal packing diagram for **1**.

change-narrowed signal in a monoclinic lattice, one of the principal directions is along the 2-fold *b* axis.

Discussion

The ground state for compounds **1** and **2** is a spin doublet delocalized on three magnetic centers and well separated in energy from the first excited states. The description of such triad states is still the subject of theoretical and experimental studies.[6-12] The knowledge of the molecular **g** tensor could provide in principle interesting information on the nature of the triad state, especially if it is possible to correlate this molecular tensor with the three local **g** tensors.[12,13] Actually, that is why we have undertaken the single-crystal EPR study reported in this note. Owing to the absence of evident intermolecular exchange pathways, we thought to obtain molecular tensors. In fact, the EPR spectra are exchange-averaged and the **g** tensors for both **1** and **2** are related to the lattice as a whole and not to the trinuclear cation. From magnetic susceptibility measurements, we have been able to estimate the magnitude J of the interaction between a molecule and its neighbor in **1**. J is found to be of the order of the wavenumber. It has been shown[4,14,15] that when the interaction between two magnetic centers noted a and b is such as

$$|J| > \tfrac{1}{2}\beta H|g_a - g_b| \qquad (6)$$

then the exchange-averaging conditions are filled. In the present case, the structure of the trinuclear cation may be schematized as and $\mathbf{g}_a$ (or $\mathbf{g}_b$) is related to the local tensors through

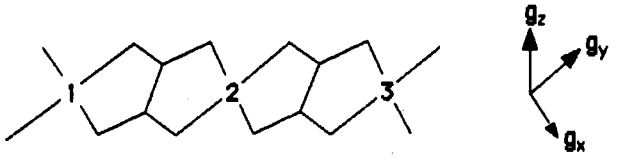

$$\mathbf{g}_a = (2\mathbf{g}_1 - \mathbf{g}_2 + 2\mathbf{g}_3)/3 \qquad (7)$$

Each copper(II) is roughly in an elongated tetragonal environment, so that its local $\mathbf{g}_i$ tensor is oriented as shown with $g_{iz} > g_{ix}$ and

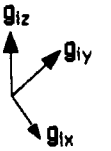

g_{iy}. It follows from (7) that $\mathbf{g}_a$ is expected to be oriented as shown at the right of the scheme of the structure. According to the crystal packing diagram[16] for **1** shown in Figure 7 and taking $g_{iz} = 2.18$ and $g_{ix} = g_{iy} = 2.07$, the largest and smallest $|g_a - g_b|$ values may be estimated as 0.026 and 0.006, respectively. It follows that $|J|$ is actually large enough to lead to exchange-narrowing effects, whatever the direction of the magnetic field may be.

In any direction of the *ac* plane for **1**, g retains a value close to the highest principal value (see Figure 3). Since the z axes perpendicular to the mean planes of the four magnetically nonequivalent trinuclear cations are almost located in this *ac* plane, this result confirms that the highest principal value of each molecular tensor is along the z direction. In other respects, although the trinuclear species in **1** and **2** are very similar, the crystal tensors are different, due to the differences of space groups and crystal packings.

A last question would deserve a comment, namely why the intermolecular interactions are so pronounced. This behavior might well be due to the presence of sulfur atoms in the periphery of the trinuclear cations and to relatively short intermolecular S···S contacts. As a matter of fact, there are several S···S contacts of the order of van der Waals radii. All involve a sulfur atom linked to the central copper and another one linked to a terminal copper. Owing to the specific diffuseness of their valence orbitals, the sulfur atoms could be involved in Cu-S···S-Cu-exchange pathways.

This work shows how one must be careful when interpreting powder EPR spectra of polymetallic species. Even if the molecular units seem to be well isolated within the crystal lattice, the spectrum may be exchange-averaged and therefore less informative than expected.

Acknowledgment. We are most grateful to Dr. F. Robert who helped us to determine the indices of the crystal faces.

(6) Figgis, B. N.; Martin, D. J. *J. Chem. Soc., Dalton Trans.* **1972**, 2174.
(7) Butcher, R. J.; O'Connor, C. J.; Sinn, E. *Inorg. Chem.* **1981**, *20*, 537.
(8) Gehring, S.; Astheimer, H.; Haase, W. *J. Chem. Soc., Faraday Trans. 2* **1987**, *83*, 347.
(9) Muhonen, H.; Hatfield, W. E. *Acta Chem. Scand.* **1986**, *A40*, 41.
(10) Journaux, Y.; Sletten, J.; Kahn, O *Inorg. Chem.* **1986**, *25*, 439.
(11) Kokoszka, G. F.; Padula, F.; Goldstein, A. S.; Venturi, E. L.; Azevedo, L.; Siedle, A. *Inorg. Chem.* **1988**, *27*, 59.
(12) Banci, L.; Bencini, A.; Gatteschi, D. *Inorg. Chem.* **1983**, *22*, 4018.
(13) Gatteschi, D.; Bencini, A. In *Magneto-Structural Correlations in Exchange Coupled Systems*; Willett, R. D., Gatteschi, D., Kahn, O., Eds.; NATO ASI Series; Reidel Publishing Co.: Dordrecht, The Netherlands, 1985.
(14) Kennedy, T. A.; Choh, S. H.; Seidel, G. *Phys. Rev. B.* **1970**, *2*, 3645.
(15) Bencini, A.; Gatteschi, D. *E. P. R. of Exchange Coupled Systems*; Springer-Verlag: Berlin, 1990, Chapter 6.
(16) The full-like Macintosh version of ORTEP was implemented by D. Andrē and A. Michalowicz and is available on request (Dr. A. Michalowicz, Laboratoire de Physico-Chimie Structurale, Universitē de Paris-Val-de-Marne, 94000 Creteil, France).

Contribution from the Sektion Chemie, Karl-Marx-Universität Leipzig, DDR-7010 Leipzig, Talstrasse 35, GDR, and Anorganisch Chemisch Laboratorium, J. H. van't Hoff Instituut, Universiteit van Amsterdam, Nieuwe Achtergracht 166, 1018 WV Amsterdam, The Netherlands

Ion-Pair Charge Transfer (IPCT) between Bipyridinium Cations and the Tetracarbonylcobaltate Anion. Spectroscopy and Thermal and Photochemical Reactions

H. Knoll,*[1a,b] R. Billing,[1a] H. Hennig,[1a] and D. J. Stufkens[1b]

Received September 1, 1989

Introduction

In recent years, increasing attention has been paid to the photochemical reactivity of coordination compounds altered in their second sphere.[2] Such changes can, e.g., be accomplished

(1) (a) Karl-Marx-Universität Leipzig. (b) Universiteit van Amsterdam.

0020-1669/90/1329-3051$02.50/0